


Continuous Inhalation Exposure to Fungal Allergen Particulates Induces Lung Inflammation While Reducing Innate Immune Molecule Expression in the Brainstem

ASN Neuro
Volume 10: 1–17
© The Author(s) 2018
Reprints and permissions:
sagepub.com/journalsPermissions.nav
DOI: 10.1177/1759091418782304
journals.sagepub.com/home/asn



Xinze Peng^{1,2,*}, Abdullah M. Madany^{1,3,4,*}, Jessica C. Jang^{4,5},
Joseph M. Valdez^{1,3,4,6}, Zuivanna Rivas^{1,4}, Abigail C. Burr⁴,
Yelena Y. Grinberg^{3,4}, Tara M. Nordgren^{1,4,7}, Meera G. Nair^{1,4,5,7},
David Cocker^{1,2}, Monica J. Carson^{1,3,4,6,7}, and David D. Lo^{1,3,4,5,7}

Abstract

Continuous exposure to aerosolized fine (particle size $\leq 2.5 \mu\text{m}$) and ultrafine (particle size $\leq 0.1 \mu\text{m}$) particulates can trigger innate inflammatory responses in the lung and brain depending on particle composition. Most studies of manmade toxicants use inhalation exposure routes, whereas most studies of allergens use soluble solutions administered via intranasal or injection routes. Here, we tested whether continuous inhalation exposure to aerosolized *Alternaria alternata* particulates (a common fungal allergen associated with asthma) would induce innate inflammatory responses in the lung and brain. By designing a new environmental chamber able to control particle size distribution and mass concentration, we continuously exposed adult mice to aerosolized ultrafine *Alternaria* particulates for 96 hr. Despite induction of innate immune responses in the lung, induction of innate immune responses in whole brain samples was not detected by quantitative polymerase chain reaction or flow cytometry. However, exposure did trigger decreases in Arginase 1, inducible nitric oxide synthase, and tumor necrosis factor alpha mRNA in the brainstem samples containing the central nervous system respiratory circuit (the dorsal respiratory group, ventral respiratory group, and the pre-Bötzinger and Bötzinger complexes). In addition, a significant decrease in the percentage of Toll-like receptor 2-expressing brainstem microglia was detected by flow cytometry. Histologic analysis revealed a significant decrease in Iba1 but not glial fibrillary acidic protein immunoreactivity in both the brainstem and the hippocampus. Together these data indicate that inhalation exposure to a natural fungal allergen under conditions sufficient to induce lung inflammation surprisingly causes reductions in baseline expression of select innate immune molecules (similar to that observed during endotoxin tolerance) in the region of the central nervous system controlling respiration.

Keywords

neuroinflammation, innate immunity, allergen, endotoxin tolerance

Received March 31, 2018; Received revised May 17, 2018; Accepted for publication May 20, 2018

¹BREATHE Center, University of California, Riverside, CA, USA

²Department of Chemical and Environmental Engineering, Bourns College of Engineering, Center for Environmental Research and Technology (Ce-Cert), University of California, Riverside, CA, USA

³Center for Glial-Neuronal Interactions, University of California, Riverside, CA, USA

⁴Division of Biomedical Sciences, School of Medicine, University of California, Riverside, CA, USA

⁵Microbiology Graduate Program, University of California, Riverside, CA, USA

⁶Neuroscience Graduate Program, University of California, Riverside, CA, USA

⁷Biomedical Sciences Graduate Program, University of California, Riverside, CA, USA

*These authors contributed equally to this work.

Corresponding Author:

Monica J. Carson, University of California Riverside, School of Medicine, 900 University Ave, Riverside, CA 92521, USA.
Email: monica.carson@ucr.edu



Introduction

For much of the 20th century, the brain was viewed as immunologically separate from the rest of the body (reviewed in Carson et al., 2006; Perry, 2010; Czirr and Wyss-Coray, 2012; Cunningham, 2013). However, triggering acute or chronic systemic inflammation with viral, bacterial, and manmade toxicants is now well described to induce innate immune responses within the central nervous system (CNS) (Perry, 2010; Cunningham, 2013; Calderón-Garcidueñas et al., 2016; Cole et al., 2016; Heusinkveld et al., 2016; Mumaw et al., 2016; Jayaraj et al., 2017; Bilbo et al., 2018; Ljubimova et al., 2018). Less studied are the neuroinflammatory consequences of airborne allergens (Klein et al., 2016).

Airborne allergens trigger both acute and chronic pulmonary inflammation and rhinitis in a large proportion of the human population at times in which the brain is still developing (childhood) through times in which the brain is at increased susceptibility for neurodegenerative disease (e.g., as with advancing age; Ghosh et al., 2013; Klein et al., 2016; Croston et al., 2018; Kader et al., 2018). Indeed, in animal model systems, chronic exposure to allergens has revealed consequences for altered behavior including impaired learning and memory in the Morris water maze, disturbed long-term potentiation in the hippocampal CA1 region, and reduced cell proliferation in the hippocampal neurogenic niche (Guo et al., 2013; Klein et al., 2016). As yet, it is unknown to what extent altered behavior might be due to innate (nonlymphocyte) immune responses versus adaptive (lymphocyte) immune responses in the CNS.

Because systemic (non-CNS) exposure to bacterial components triggers an innate (non-T cell) immune response in the CNS, it is expected that pulmonary innate immune responses to allergens would similarly trigger innate inflammation in the CNS. However, immune responses to antigens including allergens are dependent on the route of administration, the composition of the antigen, and whether antigens are administered in the presence or absence of immune activating adjuvants. In the case of antigens administered via inhalation, the size of the aerosolized particulates also can modulate the immune response (Kumar et al., 2014; Jayaraj et al., 2017; Ljubimova et al., 2018). Most studies examining the CNS consequences of allergic inflammation use neither natural allergens nor an inhalation route of exposure. Instead they most often use repetitive injections of nonallergen antigens often in the presence of adjuvants. The repetitive treatment with adjuvant-antigen cocktails is especially confounding because adjuvants by themselves can trigger neuroinflammatory responses in the CNS (Perry, 2010; Czirr and Wyss-Coray, 2012; Cunningham, 2013).

Natural allergens are characterized by multiple characteristics (Kumar et al., 2014). They are proteins often stably desiccated and delivered as part of a larger particle. They are low molecular weight, able to be eluted from the larger particle in the *wet* environment of the lung, are recognized by pathogen-associated molecular pattern (PAMP) receptors on innate immune cells, and often have protease activity. However, many studies focusing on the consequences of allergic inflammation use model systems in which the adaptive immune system (T cells) are primed to respond to a nonallergen antigen such as ovalbumin by repetitive intravenous, intraperitoneal, or subcutaneous injections in the presence of adjuvant over a period of 1 to 3 months. The allergic adaptive immune response is triggered in these model systems by subsequent acute or chronic intranasal administration of the antigen in solution (Ploix et al., 2009; Doherty et al., 2012; Klein et al., 2016; Zhou et al., 2016). Natural allergen exposure usually occurs by continuous low-dose exposure in the absence of adjuvant-based priming. Substantially, different inflammatory mechanisms are known to be triggered by this type of administration frequency than by single or multiple discrete deliveries of high antigen doses (Kumar et al., 2014; Bonam et al., 2017). Furthermore, with an intranasal treatment, the mouse is subjected to either the stress of restraint or anesthesia while held in a supine position as a micropipette is placed at the external nares and a concentrated solution is trickled slowly (Ploix et al., 2009; Doherty et al., 2012; Zhou et al., 2016). Thus, it is likely that pathologic mechanisms elicited by intranasal application (\pm sensitization) may not be representative of natural inhalation exposure to environmental airborne allergens.

Several studies have examined the consequences of inhalation exposure to natural allergens, including plant pollens, fungal allergens, and arthropod antigens, but the focus of these studies has primarily been on induction of pulmonary inflammation (Knutsen et al., 2012; Gabriel et al., 2016; Gold et al., 2017; Kubo, 2017). By contrast, most studies examining the CNS consequences of inhalation exposure have focused on the effects of airborne pollutants instead of allergens (Gackiere et al., 2011; Levesque et al., 2011; Calderón-Garcidueñas et al., 2016; Cole et al., 2016; Heusinkveld et al., 2016; Mumaw et al., 2016; Jayaraj et al., 2017; Bilbo et al., 2018; Ljubimova et al., 2018). These studies demonstrate that in the absence of priming, the inhalation route of exposure is effective at inducing both systemic and CNS inflammatory responses. While the composition of these airborne toxicants is an important determinant in triggering inflammation, particle size is also an important determinant. In animal models as well as in human epidemiological studies, it is apparent that pollutants in the fine (particle size $\leq 2.5\mu\text{m}$) and ultrafine

(particle size $\leq 0.1 \mu\text{m}$) size range are highly implicated in contributing to observed effects on the CNS.

Taken together, these types of studies have clearly demonstrated the potential for allergic responses to modify the inflammatory environment and potentially the function of the CNS. However, as yet, the CNS consequences of natural airborne allergens administered via inhalation are infrequently examined. Therefore, here we chose to test the consequences of continuous inhalation exposure to fungal *Alternaria alternata* particulates. *Alternaria alternata* is a known common allergen found to thrive on various types of vegetation. It is virtually impossible to avoid contact with *Alternaria alternata* as its spores can reach levels of thousands of spores per cubic meter of air and can be found both indoors and outdoors (Knutsen et al., 2012; Gabriel et al., 2016). As a general health risk, *Alternaria alternata* is considered one of the most abundant sources of airborne allergens, readily triggers immune sensitization and is a primary risk factor for development of asthma. Furthermore, *Alternaria alternata* exposure in previously sensitized individuals is correlated with severe increased risk of morbidity and a higher risk of fatal asthma attacks (Bush and Prochnau, 2004; Knutsen et al., 2012; Gabriel et al., 2016; Vianello et al., 2016). It is also a major allergen for asthma in children raised in desert environments and natural exposure to *Alternaria alternata* spores also induces allergic rhinitis symptoms (Halonen et al., 1997; Andersson et al., 2003; Bush and Prochnau, 2004; Knutsen et al., 2012; Gabriel et al., 2016).

Finally, studies examining the consequences of airborne exposure to manmade toxicants have demonstrated that CNS inflammation is triggered prior to the development of a mature adaptive immune response (occurring ≥ 96 hr of exposure). By contrast, studies focusing on the CNS consequences to allergens have focused primarily on the consequences of chronic or long-term inflammation comprising ongoing adaptive immune responses driving innate immune responses (Doherty et al., 2012; Ghosh et al., 2013; Kumar et al., 2014; Kubo, 2017). The type of innate inflammation induced by the initial exposure to an immune stimulant shapes qualitatively and quantitatively the subsequent T cell, B cell, and antibody responses to the initial immune stimulant (Kumar et al., 2014).

Therefore, in this study, we designed and constructed a new whole-body exposure chamber that allows us to conduct *in vivo* continuous exposure studies for inhaled toxicants. Exposure times in other model systems are often limited to repetitive short-term exposures (e.g., 4–5 hr per day for 3–5 days per week for a period up to several months; Roy et al., 2003; Roy and Pitt, 2006; McDonald et al., 2010; Barnewall et al., 2015; Ye et al., 2017). By contrast, whole-body exposures could be

continuous over days because the construction parameters of our new whole-body chamber system maintained ammonia levels well below levels required for optimal murine husbandry (Rosenbaum et al., 2009). Using this model system, we can investigate health effects of aerosolized materials without restricting animal movement or feeding behavior. This system provides controlled and well-characterized whole animal exposures where dosage is by inhalation of particle suspensions that more closely mimics natural airborne exposure in contrast to the more commonly used intranasal applications of dilute solutions of particulate material or movement-restricting nose cone administration of inhaled particulates (Roy et al., 2003, 2006; McDonald et al., 2010; Barnewall et al., 2015; Ye et al., 2017). Using this chamber, we describe the effects of continuous extended exposure to fine particle *Alternaria* allergen aerosol suspensions on inflammation in the lung and CNS. To our knowledge, this study is the first to test the consequences of this prevalent health-related airborne allergen on the brain's innate immune status. Strikingly, we find that despite inducing overt lung inflammation with eosinophilia characteristic of innate immunity preceding allergic (hypersensitivity type 1) lymphocyte responses, we did not induce proinflammatory innate immune activation with the brain (Doherty et al., 2012; Ghosh et al., 2013; Kumar et al., 2014; Kubo, 2017). Instead, we observed a decrease in basal expression of select innate immune molecules in the region of the brain regulating respiration reminiscent of the phenomenon associated with endotoxin tolerance (Nomura et al., 2000; Pena et al., 2011; Rajaiah et al., 2013; Collins and Carmody, 2015).

Material and Methods

Animals

Male C57Bl/6J mice (8–12 weeks old) were maintained in standard mouse cages with fresh bedding and standard Purina food chow for the duration of each experimental exposure. All experiments were performed in compliance with University of California Institutional Animal Care and Use Committee regulations and review.

Mouse Chamber

The chamber was made of clear acrylic sheets with internal dimensions of $40 \times 32 \times 25$ in.³ (length \times width \times height) for approximately 540 L in volume (Figure 1). Inside the chamber, two perforated aluminum plates separated the inlet (upper left) and the outlet (lower right) to enable uniform dispersion of injected aerosols. The large size of the chamber accommodates up to six mouse cages simultaneously for exposure tests. On the top of the

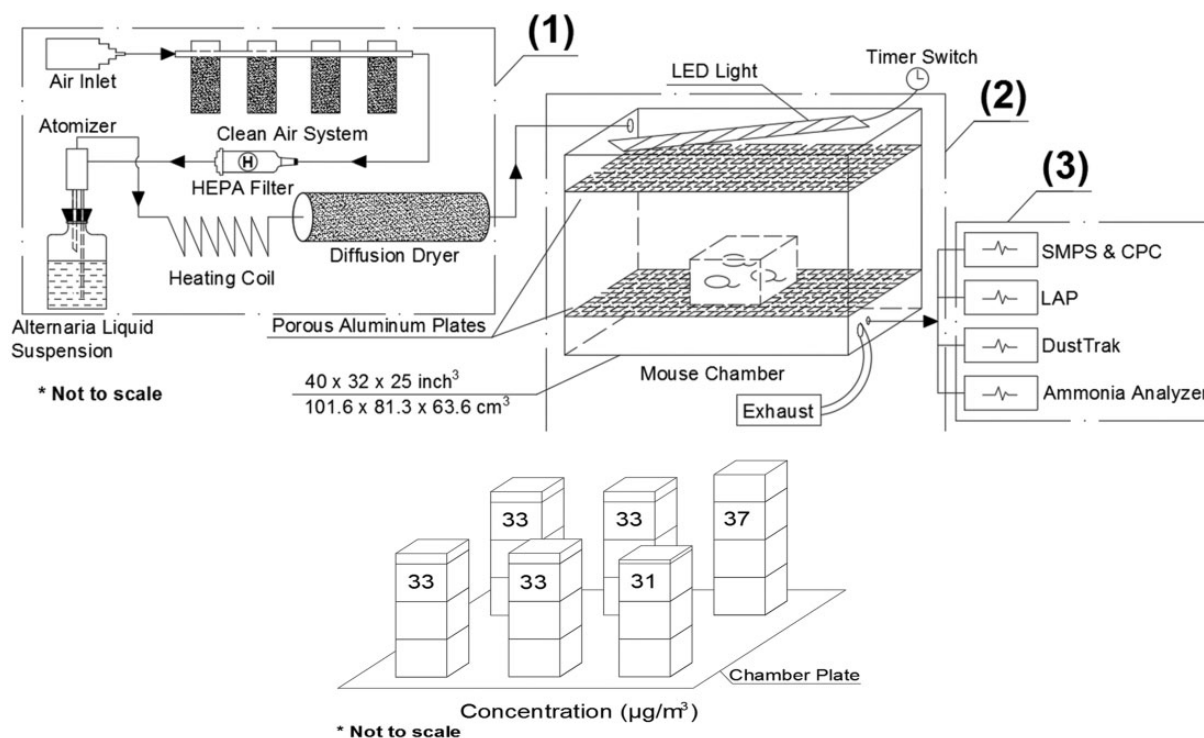


Figure 1. Exposure chamber design. (a) Schematic design of the mouse chamber system. The system includes three main components of the mouse chamber system: (1) the aerosol generation system, (2) the exposure chamber, and (3) the aerosol monitoring system. (b) Chamber characterization data: SMPS data showing distribution of particle concentrations across the chamber. HEPA = High Efficiency Particulate Air; SMPS = Scanning Mobility Particle Sizer; CPC = Condensation Particle Counter; LAP = Laser Aerosol Particle Sizer.

chamber, an LED warm light string was attached to a timer switch to provide a 12:12 hr light cycle. The whole chamber was covered with blackout cloth to ensure zero light contamination from outside. A $\frac{1}{4}$ in. inlet from the upper left of the chamber was used for injection while four $\frac{1}{2}$ in. exhaust ports located in the lower right chamber ensured that the in-chamber pressure remained the same as atmospheric. Another $\frac{1}{4}$ in. outlet located in the lower right of the chamber was used for instrument sampling and monitoring. The chamber was flushed with clean air with at least 10 chamber volumes before and after each test to avoid contamination.

Aerosol Generation

Lab compressed air passed through a clean air system consisting of silica gel (to absorb water moisture), activated carbon (to absorb organics), hopcalite (to absorb CO), and purafil (to absorb NO_x). Pressure at both the inlet and outlet of the clean air system was monitored and controlled by a pressure regulator. During the test, the inlet pressure remained controlled at 60 psi while the outlet pressure was 25 psi, resulting in an aerosol flow at 6 L/min (monitored by a mass flow controller) coming

out of the nebulizer. The nebulizer converted *Alternaria* liquid particulate solution into an aerosol spray (May, 1973) and the spray went through a diffusion dryer for physical absorption of water vapor.

Sample Monitoring System

Four instruments were attached from the sample port of the chamber. Aerosol concentration and size distribution were monitored by a Scanning Mobility Particle Sizer (SMPS). The SMPS is widely used as a standard method for the characterization of particles smaller than 1 μm in diameter (Wang and Flagan, 1990; Mulholland et al., 2006). It provides size from 2 to 1,000 nm with high resolution (107 channels). A Condensation Particle Counter was used to measure airborne particle number concentration for the SMPS to provide overall particle size distribution. The Laser Aerosol Particle Sizer served as a supplemental instrument for monitoring particle size ranging from 200 nm to 40 μm with high resolution of up to 128 channels. A DustTrak (TSI) provided information about the total PM_{2.5} concentration. A modified ammonia (NH₃) analyzer provided measurements of the NH₃ level inside the chamber.

Operation of the Chamber: Biological Material Introduction and Dose Preparation

Lab compressed air passed through a clean air system before entering an atomizer. A stainless steel atomizer generated aerosols from a 0.26 g/mL solution of *Alternaria* particulate in ultrapure water. The wet aerosol passed through a heated copper coil at 52°C to transform water moisture into vapor and the water vapor was absorbed by passing through a diffuser dryer filled with indicating silica gel, which was replaced daily. The dry aerosol was subsequently injected into the mouse chamber. The chamber held mice in conventional mouse cages with wire tops to hold food as well as enable free flow of air into the cages, and hydrogel containers in the bottom to provide water along with conventional wood shaving bedding. Injected aerosols were shown to saturate the chamber with *Alternaria* particulates by 2 hr of continuous injection. In this study, tests continued for 96 hr with continuous aerosol injection. During the injection period, instruments monitored the aerosol concentration and size distribution as well as the overall particulate matter (PM) concentration. To ensure that mice would not be affected by lung irritation from ammonia accumulation within the chamber during the time of the experiment, we used continuous air injection at a rate greater than 1 full volume change per hour. At the end of the exposure period, ammonia levels were monitored to ensure that the mice were under a nontoxic environment. The chamber was flushed with clean air of at least 10 chamber volumes before and after each test to avoid contamination.

Lung Histology and Bronchio-Alveolar Lavage Cell Counts

Bronchio-alveolar lavage (BAL) cells and fluid were recovered through intratracheal washing with 0.75 mL of ice-cold PBS as previously described (Chen et al., 2016). Cells were recovered by centrifugation followed by red blood cell lysis. BAL cells were then counted, cytocentrifuged (1,000 RPM, 5 min) onto a glass microscope slide, stained with hematoxylin and eosin (H&E), and differential counts performed based on cell morphology and stain. For each sample, >150 cells were counted from five total frames of view spread throughout the microscope slide at 40× magnification. Following BAL washing, lungs were inflated with 0.75 mL 1 part 4% PFA/30% sucrose and 2 parts OCT and stored overnight in 4% PFA at 4°C for lung histology and immunofluorescence. After 24 hr, lungs were removed from 4% PFA and incubated another 24 hr in 30% sucrose. Lungs were then blocked in OCT and sectioned at 10 μm. H&E-stained lung sections were blindly scored at 20× magnification on a 1 to 5 scale with 5 being the most severe score of pathology using criteria of leukocyte infiltration

and aggregation of leukocytes into the bronchioles (1–5) and vascular inflammation/endothelial cell hyperplasia (1–5) visualized by thickening of endothelial cells surrounding the vasculature for a total score out of 10 as previously described. Scoring of the lung section was based on the total area affected: 1, absent; 2, slight; 3, moderate (covering up to 5% of total area), 4, marked (>5% and <10% of total area), and 5, severe (covering ≥10% of total area). For immunofluorescence staining, sections were incubated with rabbit anti-resistin-like molecule alpha (RELM α) (0.5 mg/mL Peprtech), at room temperature for 2 hr. Then sections were incubated with the appropriate fluorochrome-conjugated secondary antibody for 2 hr at room temperature and counterstained with DAPI. Sections were visualized under a Leica microscope (DM5500 B).

Enzyme-Linked Immunosorbent Assay

Greiner 96-well plates were coated with primary antibodies to RELM α (Peprtech, 1 μg/mL) overnight at room temperature. After blocking the plates with 5% newborn calf serum in PBS for 1 hr, sera, BAL fluid, or tissue homogenates were added at various dilutions and incubated at room temperature for 2 hr. Detection of RELM α was done with biotinylated antibodies (Peprtech, 2.5 μg/mL) for 1 hr, followed by incubation with streptavidin-peroxidase (Jackson Immunobiology) for 1 hr in the dark. The peroxidase substrate tetramethylbenzidine (BD Biosciences) was added followed by the addition of 2N H₂SO₄ as a substrate stop, and the optical density (OD) was captured at 450 nm. Samples were compared to a serial-fold dilution of recombinant protein.

Quantitative Polymerase Chain Reaction Analysis

In brief, the medulla and the rest of the brain from each mouse were separately homogenized and total RNA was extracted using Trizol (Invitrogen, Carlsbad, CA, USA) as previously described (Hernandez et al., 2016). Following RNA extraction, first-strand cDNA was synthesized per the conditions outlined in the cDNA synthesis kit (GE Healthcare, Pittsburgh, PA, USA). Only samples with RNA and cDNA quality verified by the presence of ribosomal bands and appropriate levels of hypoxanthine guanine phosphoribosyl transferase (HPRT) transcripts per μg cDNA were used for subsequent quantitative polymerase chain reaction (qPCR) analysis. qPCR analysis was performed as previously described using a CFX96 Real Time PCR Detection System (Bio-Rad Laboratories, Hercules, CA, USA). The relative number of transcripts per HPRT transcripts was determined using calibration standards for each of the tested molecules. For each molecule being assayed, a qPCR standard curve was also generated to define the

correspondence of transcript numbers to the cycle threshold (Ct value) for qPCR detection. Specifically, standards for HPRT and each molecule being assayed were diluted to obtain standard curves of 50 pg, 5 pg, 0.5 pg, 0.05 pg, 0.005 pg, 0.0005 pg, and 0 pg (no template control) for qPCR determination of transcript levels in each sample. The transcript copy number of each molecule per sample was normalized to the expression of HPRT per sample to account for minor variations in sample aliquots. Primers for HPRT: (forward) CCCTCTGGTAGATTGTC GCTTA and (reverse) AGATGCTGTTACTGATAGG AAATCGA; Arginase 1: (forward) CAGAAGAAT GGAAGAGTCAG and (reverse) CAGATATGCA GGGAGTCACC; interleukin (IL)-6: (forward) CCCC AATTTCCAATGCTCTCC and (reverse) CGACTA GGTTTGCCGAGTA; inducible nitric oxide synthase (iNOS): (forward) GGCAGCCTGTGAGACCTTTG and (reverse) GCATTGGAAGTGAAGCGTTTC; NADPH oxidase (NOX2) (gp91-phox subunit): (forward) CCAACTGGGATAACGAGTTCA and (reverse) GAGAGTTTCAGCCAAGGCTTC; and tumor necrosis factor alpha (TNF α): (forward) CTGTGAAGGG AATGGGTGTT and (reverse) GGTCACGTG CCCAGCATCTT.

Flow Cytometry

Microglia and CNS-infiltrating macrophages were isolated from the brains and medulla oblongata of mice immediately following euthanasia as previously described (Hernandez et al., 2016). In brief, the brain with cerebellum was separated from the brainstem at the level of the border between the pons and the medulla (medulla region containing the dorsal respiratory group, the ventral respiratory group, and the Bötzing and pre-Bötzing complexes; Smith et al., 2013; Feldman and Kam, 2015). Both brain regions (the whole brain without medulla and the medulla) from each mouse were mechanically dissociated as separate samples. Samples were not pooled and were not treated with DNase or collagenase. The resulting cell suspensions were separated on a discontinuous 1.03/1.088 Percoll gradient and microglia/macrophages/infiltrating immune cells were collected from the interface as well as from the 1.03 Percoll fraction. Microglial activation was analyzed by flow cytometry using a Cell Quest-equipped FACSCalibur (BD Scientific) and fluorescently conjugated antibodies: Allophycocyanin (APC)-conjugated CD45, fluorescein (FITC)-conjugated FcR and phycoerythrin (PE)-conjugated antibodies against Triggering Receptor Expressed on Myeloid cells-2 (TREM2), Fc Receptor (FcR), CD11b, and Toll-like receptor 2 (TLR2) (BD Biosciences, San Diego, CA, USA). Microglia were defined as CD45^{lo}, FcR+ cells. Flow cytometric data were quantified using FlowJo software using standard

methodologies for identifying gated populations and mean fluorescence intensity (MFI) values (Allan and Keeney, 2010). Because baseline fluorescence values are not absolute values between experiments, all MFI values were normalized to untreated male mice. MFI values for the CD45^{lo}, FcR+ cell population were calculated for each activation marker using FlowJo software.

Histology

Brain tissue collected at dissection was immediately incubated at 4°C for 24 hr in 4% paraformaldehyde, followed by 48 hr in 4% paraformaldehyde/30% sucrose solution. Tissue was cryopreserved, cryosectioned (25 μ m) onto Fischer Superfrost plus slides and exposed to rabbit anti-Iba1 antibodies (Wako) and murine anti-gial fibrillary acidic protein (GFAP) antibodies (Invitrogen Thermofisher), followed by incubation with Alex-680 conjugated goat anti-rabbit and Alexa-488 conjugated goat anti-mouse antibodies (Invitrogen Thermofisher) as previously described (Ploix et al., 2011). Tissue sections were mounted in Prolong Gold containing DAPI and subsequently imaged on a Yokogawa spinning disc confocal microscopy system. Immunofluorescence was quantified (6 mice per condition, 2 brain sections per mouse) with NIH Image J (version 1.5K) using the Mean Gray Value tool (sum of the gray values of all pixels in specific fluorescent channel divided by the number of pixels in the specific fluorescent channel in the total image). Specifically, the CA1 region of the hippocampus in the stratum radiatum (−1.5 to −2.5 mm past bregma on a sagittal plane) and the dorsal medulla, ventral to the fourth ventricle (−5.5 to −6.5 mm past bregma on a sagittal plane).

Statistical Analysis

Values are reported as means \pm standard error of the mean (*SEM*), with sample size as reported in each assay. Student's *t* test or analysis of variance (ANOVA) with post-hoc Dunnett's multiple comparison test were used to analyze data as indicated using Prism7 (Graphpad Software, La Jolla, CA). No significant differences were detected in the standard deviation of populations being compared by ANOVA (Brown-Forsythe test $p = .9516$). In all data sets, sample comparisons with *p* values less than .05 were considered statistically significant.

Results

Production of Stable Aerosol Suspensions of *Alternaria* Nanoparticles in an Environmental Chamber

Here, we report a mouse environmental chamber able to provide continuous air injection with the capability

to inject a stable suspension of particulates or other aerosol components over an extended period (Figure 1). Figure 1(a) depicts the chamber system and Figure 1(b) depicts representative TSI DustTrak data showing relatively even distribution of test particles across the chamber. The chamber and injection characteristics were subsequently characterized along several parameters, including aerosolized particle size and concentration, stability in aerosol suspension within the chamber, and ammonia levels (Figures 2 and 3). Specifically, aqueous solutions of *Alternaria* particulate at different concentrations were injected through an atomizer and the resulting aerosolized particle suspension was analyzed. The concentration of particles in the chamber was dependent on the *Alternaria* solution concentration (Figure 2(a)).

To characterize the stability of the particle suspension, several studies were conducted with no mice present in the chamber while particle concentration and distribution were monitored using the SMPS system. Particles in the chamber were found to show an average peak particle size of approximately 100 nm regardless of the concentration of aqueous solutions of *Alternaria* particulate (Figure 2(a)) or the presence of mice in the chamber (Figure 2(b)). Figure 2(a) and (b) also shows that the average particle number concentration of two separate injections of aqueous solution (0.26 g/L) in the chamber were nearly identical with or without the presence of mice. The mass concentration of the particles in the chamber under continuous injection conditions remained relatively stable overtime with the slight variations possibly reflecting minor variation in air pressure in the injection system (Figure 2(c)). While there was a range of particle sizes (Figure 2(a) and (d)), the average particle size appeared to be a property of the *Alternaria* particulate rather than the concentration of the protein. Thus, as with the comparisons between empty chamber and the chamber with mice, the chamber conditions did not affect the particle size, concentration, or stability.

To confirm that appropriately low ammonia levels were maintained for the duration of an experimental exposure treatment, we measured ammonia within the chamber at the end of a full 96-hr exposure (Figure 3). Although precise upper limits for murine exposure are debated, it has been generally accepted that human exposure limits should not be exceeded for laboratory-housed rodents with 25 parts per million being the recommended exposure limit as an 8-hr time-weighted average according to National Institute for Occupational Safety and Health guidelines (Rosenbaum et al., 2009). Here, we found that ammonia levels were significantly lower than the recommended 25 parts per million even with six mice in the chamber (levels were <200 parts per billion).

Continuous Exposure to *Alternaria* Particulate Nanoparticles Induces Overt Pulmonary Inflammation

We initially quantified lung inflammation by standard bronchio-alveolar lavage (BAL) and histology as the first site of allergen exposure (Figure 4). We found that 96 hr of treatment was insufficient to trigger a statistically significant increase in numbers of immune infiltrates in BAL with a standard regimen of daily intranasal dosing of the *Alternaria* particulate solution (Figure 4(a) to (c), blue bars). By contrast, 96 hr of continuous chamber exposure to aerosolized *Alternaria* particulates was sufficient to cause significant (~60%) increases in the numbers of total lavage cells (Figure 4(a), red bar; $F=8.853$, $p=.0162$) and in total alveolar macrophages (Figure 4(b), red bar; $F=9.314$, $p=.0145$). While inhalation exposure was more effective at triggering immune cell influx into the lung, histological analysis revealed that both the intranasal dosing regimen and continuous chamber exposure to aerosolized *Alternaria* particulates triggered similar degrees of total lung pathology (Figure 4(d) and (e)). Specifically, blinded scoring of histology confirmed inhalation exposure to *Alternaria* particulates induced airway and endothelial thickening equivalent to that induced by conventional intranasal administration ($F=14.54$, $p=.0003$). Immunofluorescent staining for RELM α , a highly expressed protein in asthmatic inflammation (Doherty et al., 2012), revealed that both intranasal and inhalation exposure to *Alternaria* induced modest expression in the airway and in the lung parenchyma (Figure 4(c)). Quantification of RELM α induction in lavage-isolated cells by Enzyme-Linked Immunosorbent Assay revealed no significant differences between treated and untreated groups (Figure 4(d)). Together, these studies show that physiological exposure to *Alternaria* particles in the form of aerosols in an atmospheric chamber is sufficient to produce pulmonary inflammation exhibiting early signs of allergic-type innate immune responses.

Inhaled *Alternaria* Exposure Decreases Basal Level of Innate Immune Molecules in Brain Medulla

We hypothesized that if continuous inhalation exposure to *Alternaria* particulates was sufficient to trigger lung inflammation, it should also be sufficient to trigger neuroinflammatory responses within the brain. Therefore, we surveyed the expression of molecules previously implicated in systemic- and emission particle-induced innate immune responses: Arginase 1, iNOS, NOX2, TNF α , and IL-6 (Figures 5 and 6). Surprisingly, an initial qPCR survey detected no significant differences in the expression of these molecules in cDNA prepared from total brain tissue of mice plus/minus *Alternaria* exposure (Figure 5). In the absence of global differences detectable

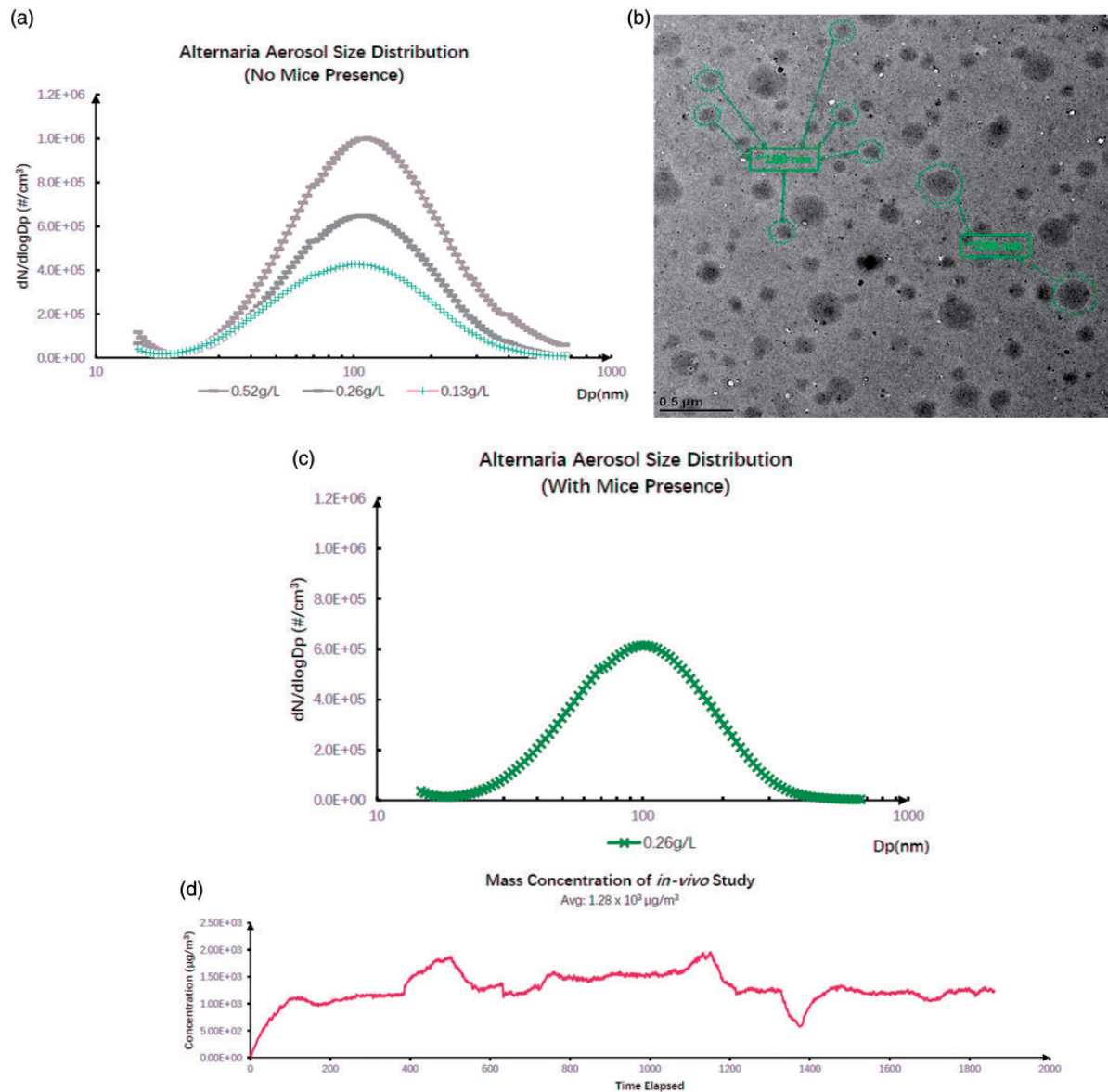


Figure 2. *Alternaria* aerosol particle size distribution (with and without mice) in the chamber. (a) Illustration of *Alternaria* aerosol particle size distribution and concentration at bottle solution of 0.13 g/L, 0.26 g/L, and 0.52 g/L, respectively. The vertical axis for represents particle number concentration $dN/d\log D_p$ ($\#/cm^3$), while the horizontal axis represents particle size on a logarithmic scale. (b) The overall size distribution during the test with mice presence over 96 hr. (c) Illustration of the mass concentration over the 96-hr exposure. (d) TEM image of the distribution of nebulized *Alternaria* aerosol particles (sampled through a low-pressure impactor that collects particles ranging from 50 nm to 4 μm) on a carbon-coated copper grid (Hering et al., 1978). TEM = transmission electron microscopy.

in total brain samples, we speculated that any effects in the CNS might be localized to specific brain regions. We chose to examine the brain region involved in the direct innervation and regulation of respiration (Smith et al., 2013; Feldman and Kam, 2015). For all subsequent experiments, we dissected the medulla containing the *CNS respiratory circuit* (composed of the dorsal respiratory group, the ventral respiratory group, and the Böttinger and pre-Böttinger complexes) away from the rest of the brain (Figure 6).

While no significant difference in Arginase 1 and iNOS expression levels was detected in cDNA from the whole-brain samples of naïve and *Alternaria*-exposed mice (Figure 5(a) and (b)), both arginase 1 (Figure 6(a); $t=3.434$, $df=20$) and iNOS levels (Figure 6(b); $t=2.293$, $df=20$) were significantly decreased by $\sim 50\%$ in cDNA from the medulla of *Alternaria*-exposed mice as compared to cDNA from the medulla of naïve mice. Arginase 1 and iNOS both compete for the same substrate: arginine. Arginase

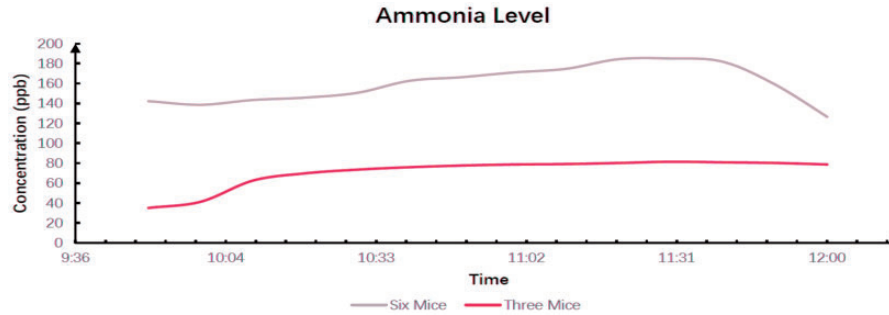


Figure 3. Ammonia level in the end of the 96-hr exposure. The ammonia gas (NH_3) concentration in the chamber was acquired at the end of each 96-hr exposure experiment. The figure shows two different ammonia (NH_3) levels during the last 3 hr of an exposure study with either three (dashed black line) or six (solid blue line) mice in the chamber.

converts arginine to ornithine leading to the polyamine pathways while iNOS generates nitric oxide from arginine. Thus, the ratios of arginase 1 to iNOS are often used as a diagnostic marker of a shift in innate immune propensity for anti-inflammatory/tissue repair responses to a propensity for proinflammatory cytotoxicity responses (Munder et al., 1998; Gordon, 2003; Cho et al., 2014). Therefore, we also compared the ratios of Arginase 1/iNOS per mouse as a measure of altered polarization separate from the absolute levels of each transcript. Exposure to aerosolized *Alternaria* particulates did not cause significant changes in Arginase 1/iNOS ratios in either the brain as a whole or in the medulla (Figures 5(c) and 6(c)). NADPH oxidase (gp91-phox subunit: NOX2), $\text{TNF}\alpha$, and IL-6 are classic proinflammatory molecules induced in the CNS by systemic inflammatory challenges and by CNS injury (Figure 6(d) to (f)). While no difference in NOX₂ and IL-6 expression was observed between the *Alternaria* and ambient air-exposed mice (Figure 6(d) and (f)), the mean baseline levels of $\text{TNF}\alpha$ were reduced by nearly 66% in the medullas of *Alternaria*-exposed mice (Figure 6(e); $t = 2.090$, $df = 20$).

Inhaled *Alternaria* Exposure Decreases Percentage of Microglia Expressing Detectable TLR2

Systemic inflammation as well as inhaled pollutants can trigger infiltration of peripheral immune cells into the CNS with even small (fine and ultrafine) particulates in the size range, but with different composition than the *Alternaria* particulates used here (Jayaraj et al., 2017). The most quantitative method for characterizing the degree of immune cell influx is flow cytometric analysis of CD45⁺ cells (Carson et al., 2006). In brief, all nucleated cells of hematopoietic origin including microglia express CD45 (also known as leukocyte common antigen). However, microglia express very low levels of CD45 (CD45^{lo}) while all other differentiated immune cells in the adult express an order of magnitude higher

CD45 levels (CD45^{hi}). In cell suspensions of the brain and medulla, microglia are identified as FcR⁺ (Figure 7(a), FL1-H) and CD45^{lo} (Figure 7(a), FL4-H). In all samples from naïve and *Alternaria*-exposed mice (brain: Figure 7(a) and (b) and medulla: Figure 7(c)), no CD45^{hi} cells were detected (Figure 7(a) to (c)). Thus, there was no overt peripheral immune cell infiltration in *Alternaria*-exposed mice despite ongoing inflammation in the lung (Figure 4(a)).

By immunolabeling with PE-conjugated antibodies, we analyzed microglial surface expression of PAMP receptors (CD11b, TLR2, and TLR4) which have been implicated in neuroinflammatory responses to systemic inflammation and inhaled pollutants (Jayaraj et al., 2017). We also examined microglial expression of TREM2 as a marker of general microglial activation. TREM2 expression is often induced by brain injury while its expression is reduced by direct exposure to LPS and TNF (Schmid et al., 2009). In the brain (Figure 7(b)) and in the medulla (Figure 7(c)) of naïve mice, nearly 100% of microglia express CD11b (blue population is CD11b⁺, nonspecific autofluorescence is gray population, Figure 7(b) and (c)). Moreover, 96-hr treatment with aerosolized *Alternaria* particulates did not alter the percentage of microglia expressing CD11b, TLR4, or TREM2 in either brain or medulla cell suspensions (Figure 7(d), (f), (j), (l), (m), and (r)). By contrast, the percentage of TLR2⁺ microglia in medulla cell suspensions was decreased by ~30% in *Alternaria*-exposed mice as compared to naïve mice (Figure 7(p)). However, the level of TLR2 per TLR2⁺ microglia (MFI per microglia) was not altered by *Alternaria* exposure (Figure 7(q)). While the percentage of CD11b⁺ cells was not altered by *Alternaria* exposure, CD11b levels per cell were increased by *Alternaria* exposure in both the whole brain (Figure 7(e)) and in the medulla (Figure 7(m)). Although quite modest and of uncertain biologic significance, chamber exposure did reduce TREM2 levels per microglia in the medulla (Figure 7(o)).

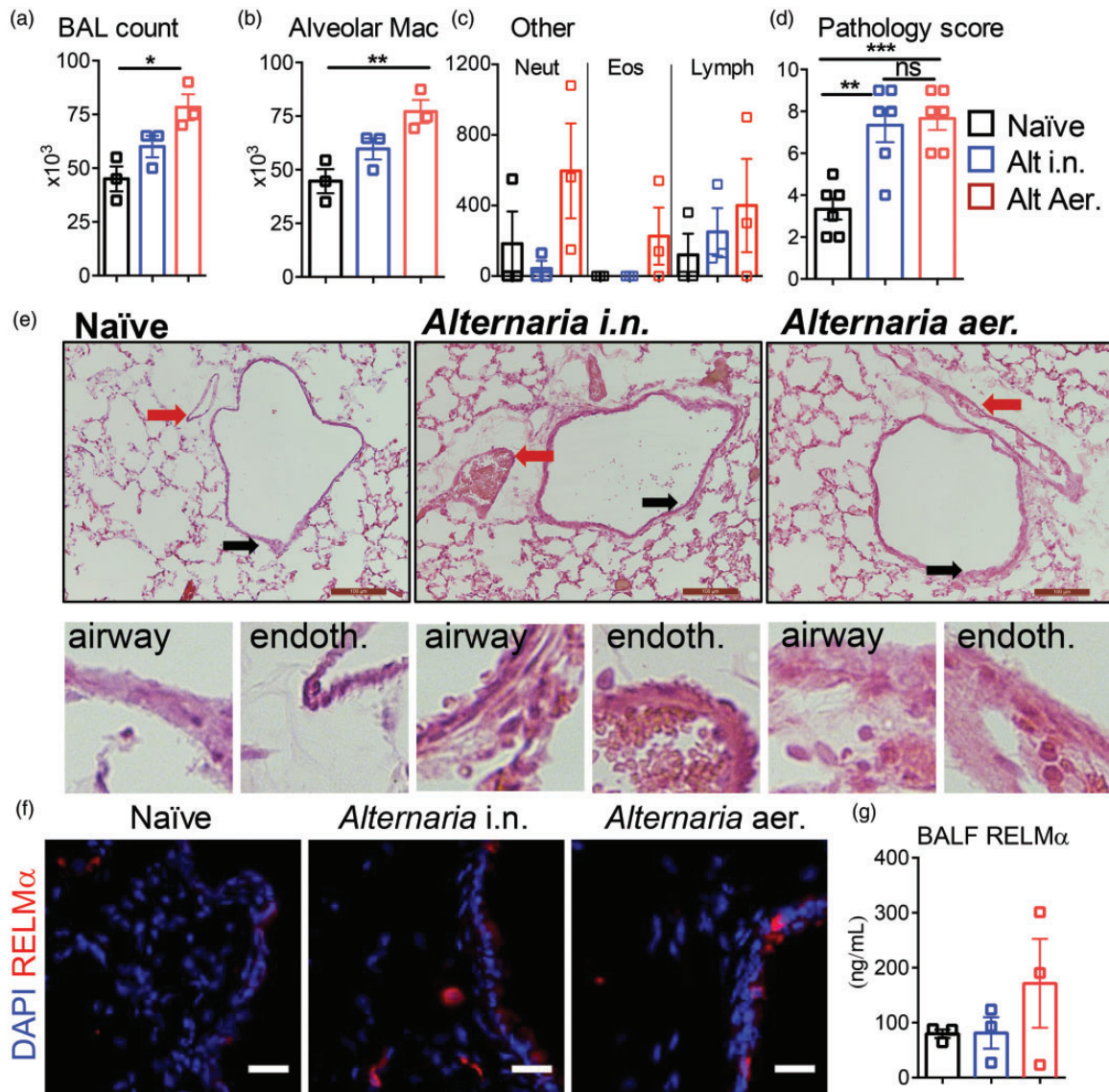


Figure 4. *Alternaria* aerosol exposure in the environmental chamber promotes lung inflammation. Bronchio-alveolar lavage (BAL) of the lungs reveal *Alternaria*-induced cell numbers (a); alveolar macrophages (b); neutrophils (Neut), eosinophils (Eos), and lymphocytes (Lymph) (c); and lung pathology scores (d). (d) Representative H&E-stained lung sections reveal *Alternaria*-induced airway (black arrow) thickening and endothelial (red arrow) thickening and inflammation (scale, 100 μ m). (f) Immunofluorescence labeling reveals increased expression of RELM α following *Alternaria* exposure (scale, 25 μ m). (g) BAL Enzyme-Linked Immunosorbent Assay for RELM α . Three biologic replicates per experiment (total of two experiments) were analyzed for each condition depicted. Data are presented as mean \pm SEM. Statistical differences were calculated by one-way ANOVA with post hoc Dunnett's multiple comparison test using GraphPad Prism. * $p < .05$. BAL = bronchio-alveolar lavage.

Inhaled *Alternaria* Exposure Decreases *Iba1* but Not GFAP Immunoreactivity

Within the CNS, *Iba1* is expressed by microglia and GFAP by astrocytes. Prior to our studies, Klein et al. (2016) challenged mice with a natural allergen from timothy grass and observed a decrease in hippocampal microglial activation using histologic measures. However, their methodology included repetitive administration of the natural allergen as a solubilized antigen

preceded by adjuvant priming. Therefore, it is unclear whether the reduced microglial reactivity was due to a mature lymphocyte response that evolved over weeks or the repetitive route of administration. Here, we compared *Iba1* and GFAP immunofluorescence in the medulla (Figure 8(a) and (b)) and hippocampus (Figure 8(c) and (d)) of mice exposed to ambient air (naïve, Figure 8(a) and (c)) or aerosolized *Alternaria* particulates (chamber, Figure 8(b) and (d)) for 96 hr. Microglia and astrocytes in *Alternaria*-exposed mice retained the

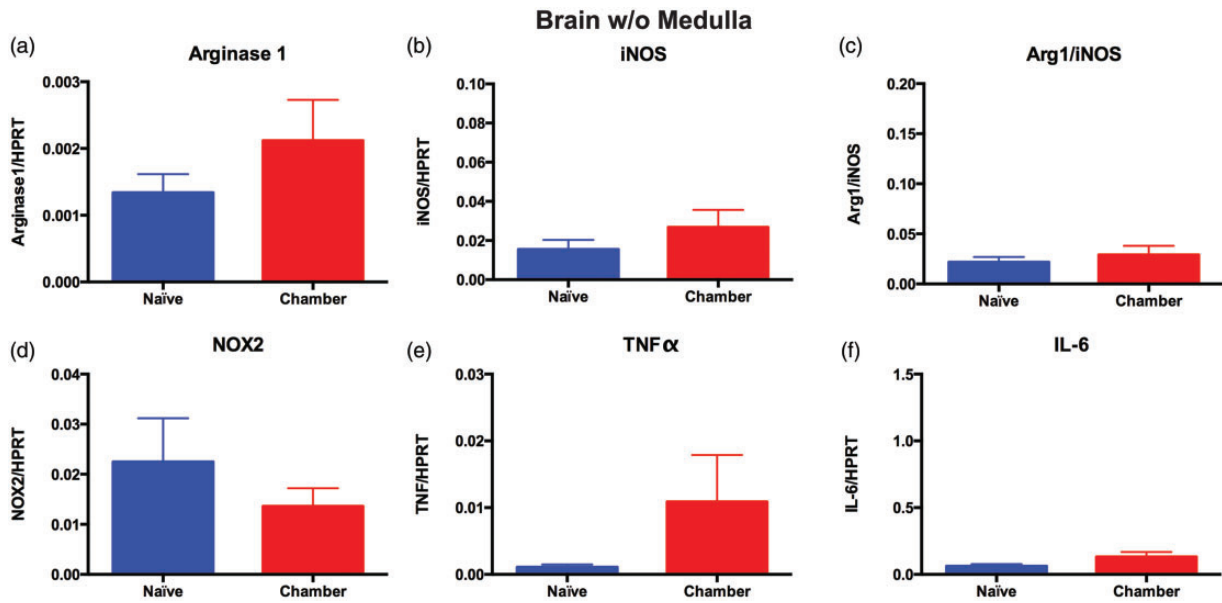


Figure 5. qPCR analysis of neuroinflammatory molecules in brain cDNA from mice exposed for 96 hr to aerosolized *Alternaria* particulates or ambient air. (a–f) Data from samples of whole brain with the medulla removed. Data are presented as the mean \pm SEM of three independent experiments with a total sample size of naive $n = 15$ and chamber (*Alternaria*-exposed) $n = 15$. Statistical differences were calculated by unpaired Student’s t test using GraphPad Prism. $*p < .05$. iNOS = inducible nitric oxide synthase; NOX2 = NADPH oxidase; TNF- α = tumor necrosis factor alpha; IL-6 = interleukin-6.

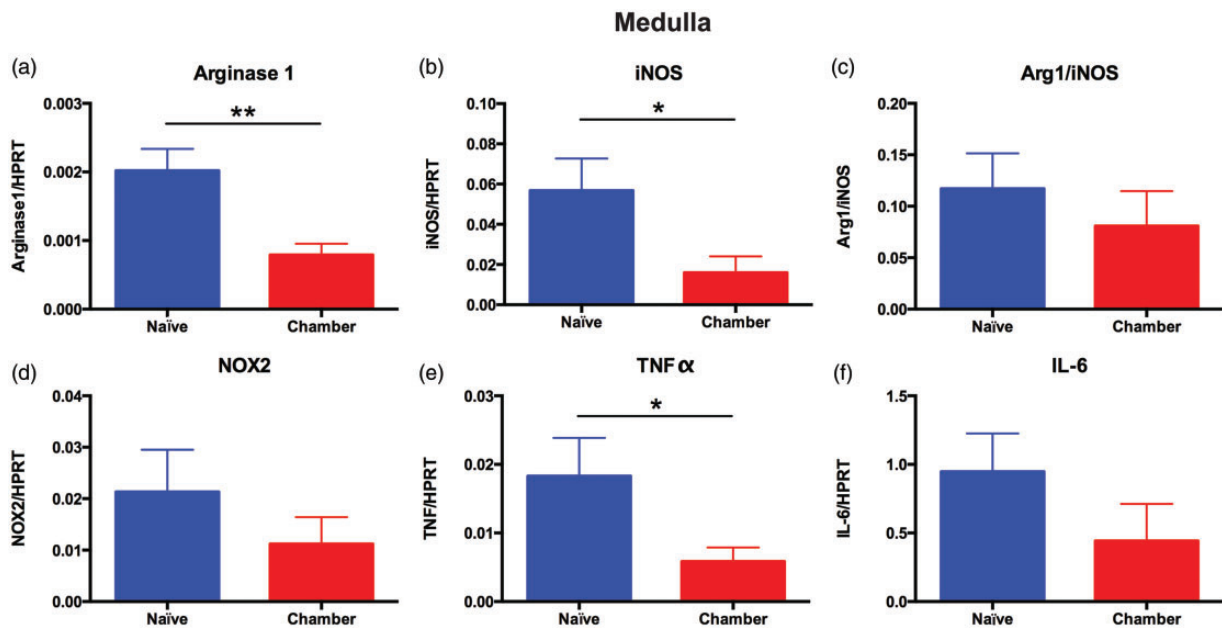


Figure 6. qPCR analysis of neuroinflammatory molecules in brain medulla cDNA from mice exposed for 96 hr to aerosolized *Alternaria* particulates or ambient air. (a–f) Data from samples of brain medulla (containing the dorsal respiratory group, the ventral respiratory group, and the Bötzing and pre-Bötzing complexes implicated in regulating lung respiration). Data are presented as the mean \pm SEM of three independent experiments with a total sample size of naive $n = 15$ and chamber (*Alternaria*-exposed) $n = 15$. Statistical differences were calculated by unpaired Student’s t test using GraphPad Prism, $*p < .05$. iNOS = inducible nitric oxide synthase; NOX2 = NADPH oxidase; TNF- α = tumor necrosis factor alpha; IL-6 = interleukin-6.

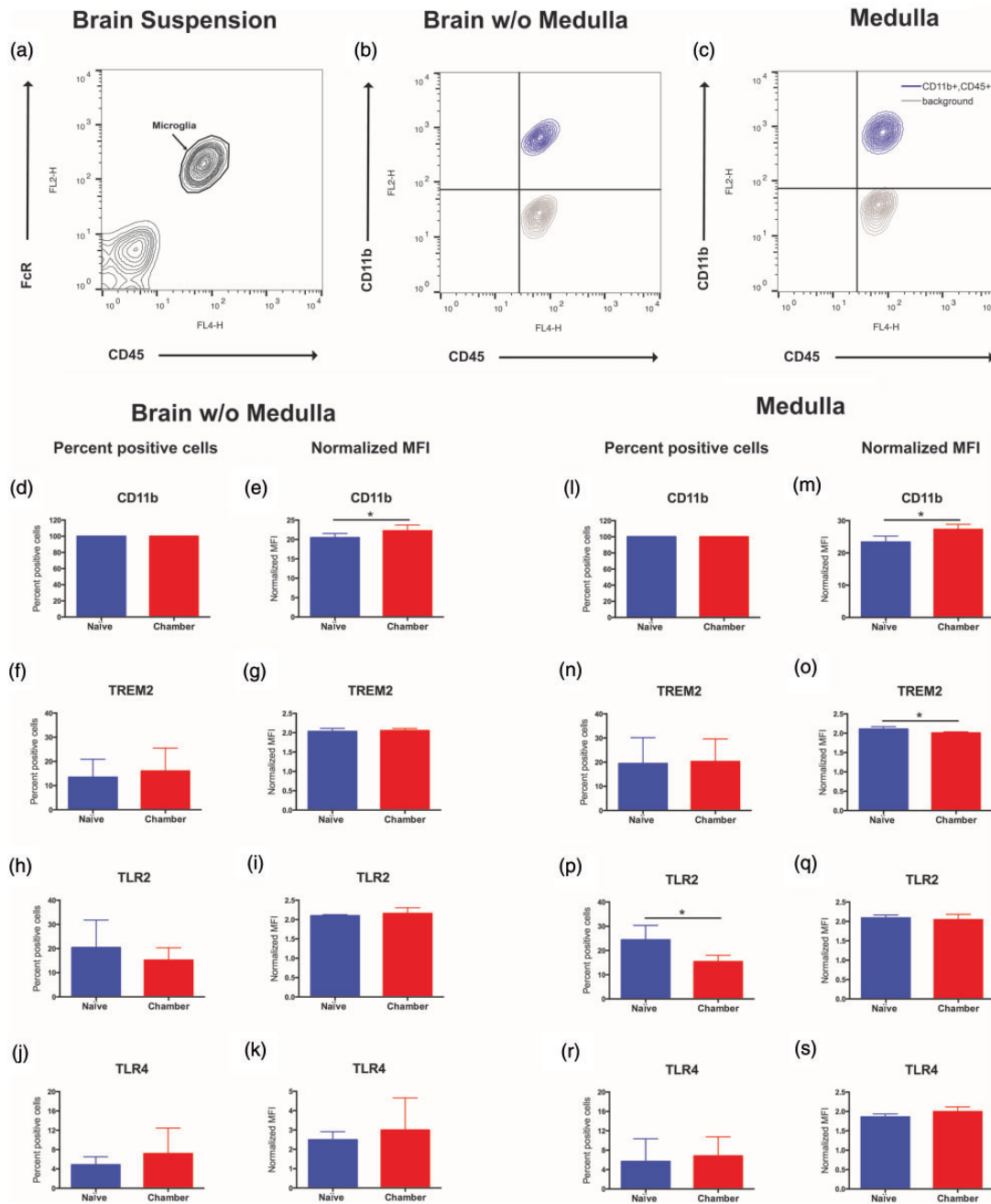


Figure 7. Flow cytometric analysis of microglial innate immune markers in brain and medulla cell suspensions from mice \pm exposure for 96 hr to aerosolized *Alternaria* particulates. (a) Representative contour plot data of brain cell suspensions labeled with FITC-conjugated anti-FcR antibodies (FL1-H) and APC-conjugated anti-CD45 antibodies (FL4-H). The FcR⁺ and CD45^{lo} microglial population is identified by the arrow. Representative contour plot data from brain cell suspensions labeled with are depicted from cell suspensions of brain w/o medulla (b) and of the medulla only (c). Cell suspensions labeled only with FITC-conjugated FcR antibodies and APC-conjugated anti-CD45 antibodies are depicted in gray and depict the relative level of autofluorescence in the FL-2 PE channel. Cell suspensions labeled additionally with PE-conjugated anti-CD11b antibodies are depicted in magenta. Cell suspensions from brain without medulla (d to e) and from only medulla (l to s) were similarly labeled with PE-conjugated antibodies against TREM2, TLR2, and TLR4. The percentages of microglia being immunoreactive for each molecule above background fluorescence (background: gray population in (b) and (c)) and the mean fluorescence intensity (relative expression level per microglia) were calculated in FlowJo and graphed in Graphpad Prism. Data are represented as mean \pm SEM from a total sample size of $n = 6$ (all parameters for brain without medulla) and $n = 4$ (for all medulla samples). Statistical differences were calculated by unpaired Student's *t* test using GraphPad Prism, * $p < .05$. Student's *t*-test values: (e) $t = 0.5186$, $df = 10$; (m) $t = 3.246$, $df = 6$; (p) $t = 2.765$, $df = 6$. TREM2 = triggering receptor expressed on myeloid cells-2; TLR = toll-like receptor.

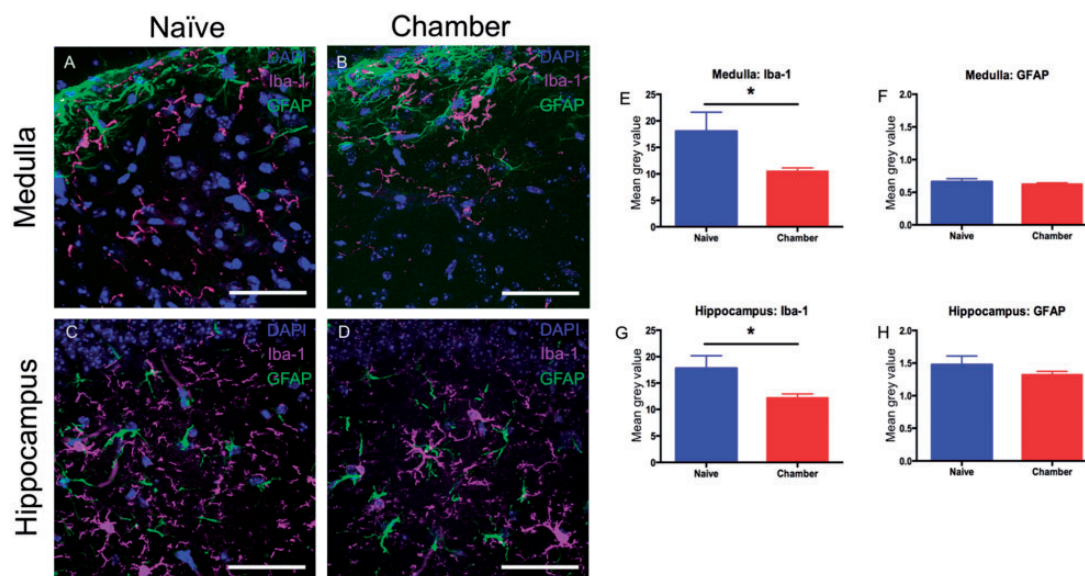


Figure 8. Histological analysis of microglia and astrocytes in tissue from mice \pm exposure for 96 hr to aerosolized *Alternaria* particulates. Glial immunofluorescence was examined in medulla (a and b) and hippocampus (c and d) from mice exposed to ambient air (a and c) or aerosolized *Alternaria* particulates (b and d). In (a) to (d), nuclei were labeled with DAPI (blue), microglia with Iba-1 antibodies (magenta) and astrocytes with anti-GFAP antibodies (green). Immunofluorescence was quantified using NIH image J (e and h) and data are represented as mean \pm SEM from a total sample size of $n = 6$ (ambient air) and $n = 6$ (*Alternaria*-exposed). Statistical differences were calculated by unpaired Student's *t* test using GraphPad Prism, $*p < .05$. Iba-1 Student *t* test values: hippocampus— $t = 2.241$, $df = 10$; medulla— $t = 2.270$, $df = 10$.

characteristic stellate morphology observed in ambient air-exposed mice. However, the mean immunofluorescence of Iba-1 per image was significantly reduced by nearly 50% in the hippocampus of *Alternaria*-exposed mice and by nearly 30% in the medulla (Figure 8(e) and (g)). By contrast, mean immunofluorescence of GFAP per image was not significantly reduced (Figure 8(f) and (h)).

Discussion

Exposure to airborne particulates (natural and man-made) is a major focus for understanding environmental contributions to the pathogenic mechanisms underlying asthma, cardiovascular disease, and neurodevelopmental and neurodegenerative disorders (Dockery et al., 1993; Kodavanti et al., 2000; Pope et al., 2002; Kodavanti et al., 2011; Raaschou-Nielsen et al., 2013). A central theme in epidemiologic and mechanistic studies defining disease-promoting contributions has been to define the links between air exposures and organ-specific inflammatory responses likely to provoke maladaptive or disease-predisposing conditions in lung, heart, and brain (Gackiere et al., 2011; Levesque et al., 2011; Calderón-Garcidueñas et al., 2016; Cole et al., 2016; Heusinkveld et al., 2016; Mumaw et al., 2016; Jayaraj et al., 2017; Bilbo et al., 2018). Allergic lung inflammation is known to cause systemic and organ-specific inflammation

(Xia et al., 2014). Therefore, based on studies defining the effects of ambient manmade airborne toxicants and systemic inflammation inducing activation of CNS innate immune responses, it is possible that natural allergens could also have detrimental effects predisposing the brain for disease-predisposing conditions.

Studies examining the effects of natural allergens including plant pollens, fungal allergens, and arthropod antigens have focused primarily on defining mechanisms of allergic lung inflammation and propensity for chronic pulmonary diseases such as asthma (Doherty et al., 2012; Gabriel et al., 2016; Knutsen et al., 2012; Gold et al., 2017; Kubo, 2017). The few reports linking allergic lung inflammation and neuroinflammation have not examined ambient exposure of allergens. Instead, these reports have relied on immune sensitization protocols often in the presence of robust adjuvant-based priming of allergic inflammation using well-characterized antigens such as ovalbumin which lack the defining features of an allergens (Xia et al., 2014; Yamasaki et al., 2016). Most studies with nonallergen antigens observed induction of proinflammatory innate immune responses in the brain (Sarlus et al., 2013; Yamasaki et al., 2016). However, one study that did examine the consequences of a natural allergen from Timothy grass looked at only the long-term neuroinflammatory consequences of allergic inflammation stimulated by a solubilized antigen administered in a long-term injection priming/intranasal

challenge model system. Striking in this system, microglial activation was reduced in specific regions of the brains from treated mice (Klein et al., 2016). These studies have been useful in defining the potential of allergic inflammation to drive neuroinflammation but have also provided potentially conflicting results. In part, this may be because these studies rely on strategies that may induce hypersensitivity immune responses that are unrelated to natural allergens associated with unprimed exposure to allergens by continuous period of inhalation (Kumar et al., 2014). In addition, these studies have primarily examined long-term allergic responses (>12 weeks of fully developed respiratory asthma with fully developed adaptive immune responses; Xia et al., 2014; Klein et al., 2016).

In our current studies, we sought to use an experimental system that mimics chronic environmental exposure to aerosolized particulates. Therefore, we generated and characterized a novel murine exposure chamber equipped to disperse a natural fungal allergen continuously and simultaneously to monitor sustained aerosolized dispersion of the natural allergen. Specifically, our chamber is much larger (540 L) than other reported chamber systems with (0.4 L or 16 L volumes) and thus able to house up to 18 mice at a single time without accumulation of high ammonia levels (Barnewall et al., 2015; Ko et al., 2015). Our chamber system also uses multiple instruments to characterize particle sizes ranging from 2 nm to 40 μm , instead of using only one instrument to detect particles in the range of 500 nm to 20 μm (Barnewall et al., 2015). In contrast to nose-only exposure systems that limits the animal activities and only allow 2-hr exposed time for each test, our chamber system allows continuous exposure to occur under conditions of free mobility and normal access to food and water (Ye et al., 2017).

It is difficult to determine the actual absorbed dose of allergen in the lung, whether it is applied intranasally or intratracheally as a solution or as a nebulized aerosol. In this study, we chose a stable aerosol suspension concentration, which we could set by using a fixed *Alternaria* particulate concentration at the atomizer (in this case, 0.26 g/L). Thus, for each exposure study, mice were placed in the chamber and the aerosol injection was begun, and particle concentration and size were monitored to ensure a stable suspension. This exposure was continued for 96 hr because 96 hr encompasses the entire period of initial innate immune response to the allergen and after which lymphocytic responses to the allergen become apparent. The nebulized *Alternaria* aerosol particles were found to be an average size of approximately 100 nm. This size range is within the size ranges of ultrafine $\text{PM}_{0.1}$ and fine $\text{PM}_{2.5}$ particles of airborne toxicants demonstrated to provoke potent inflammatory responses. Indeed, such fine aerosol particles are capable

of penetrating deep into the alveolar spaces in the lung (Barnewall et al., 2015; Jayaraj et al., 2017). Therefore, continuous exposure to aerosolized *Alternaria* particulates ensured wide distribution throughout the lung and avoided the known artefactual ingestion of a large proportion of an allergen solution when applied intranasally. In addition, continuous exposure over several days avoided the immunoregulatory effects of inducing multiple short-term bursts of acute systemic allergic hypersensitivity responses.

Proinflammatory innate immune responses are triggered within the CNS by systemic inflammation induced by bacterial and viral stimuli as well as by sustained exposure to airborne emission particulates in the size range of the *Alternaria* particles used here (Jayaraj et al., 2017).

In our model system, we were struck by the ability of continuous inhalation of aerosolized *Alternaria* particulates to drive lung inflammation that was more robust than daily intranasal application of an *Alternaria* particulate solution. Furthermore, it was notable that simple continuous inhalation exposure without prior antigen sensitization and without the inclusion of priming adjuvant was by itself sufficient to drive a large BAL inflammatory infiltrate comprising a mixed population of macrophages, neutrophils, and eosinophils characteristic of allergic responses. Therefore, it might be surprising or alternatively it might be comforting that broad-spectrum proinflammatory responses were not observed in the brain after exposure to this common natural airborne fungal antigen in the presence of robust lung inflammation. However, the study by Klein et al. (2016) does suggest that natural allergens albeit using an adjuvant priming/challenge model resulted in decreased microglial activation as assayed by histologic measures. Because mature Th2/IgE lymphocyte responses were fully developed at the 12-week time point of their assay collection, the authors ascribed the reduction in microglial activation to the sustained actions of a fully mature adaptive immune response. Here, we report observations in the brainstem and hippocampus consistent with their study (decreased Iba1 immunofluorescence, decreased expression of a subset of innate immune markers) prior to the development of a fully mature lymphocyte and IgE allergy response.

When considering the apparent lack of proinflammatory responses in the brain, it is useful to place our observations in the context of endotoxin tolerance (also referred to as LPS preconditioning; Nomura et al., 2000; Pena et al., 2011; Rajaiah et al., 2013; Collins and Carmody, 2015). Endotoxin tolerance refers to the well-described phenomena where pretreatment of immune cells or of an individual with a series of low-dose endotoxin (lipopolysaccharide) treatments causes the cells or individual to become refractory to subsequent

endotoxin challenge. Phenotypically, macrophages treated to become endotoxin tolerant express lower levels of many proinflammatory and PAMP receptor molecules at baseline prior to subsequent endotoxin challenge. Indeed, initial reports have ascribed endotoxin tolerance to the acquisition of an alternatively activated (M2) innate immune status. In our studies, we did indeed see decreased expression of TNF α and iNOS in brainstem tissue samples as well as decreased expression of TLR2 on brainstem microglia. While these are indicative of a lower propensity for a proinflammatory response to immune stimulants, a shift toward an alternative or M2-polarized phenotype should result in an altered ratio of key innate immune markers. Specifically, an alternative activation/M2 baseline polarization should have been reflected in an increased Arginase1/iNOS ratio which we did not observe (Munder et al., 1998; Gordon, 2003; Cho et al., 2014). More recently, the association of endotoxin tolerance with acquisition of an alternative/M2 innate immune polarization is being revisited as in many paradigms Arginase 1 is decreased as observed in our studies (Rajaiah et al., 2013).

Changes in baseline innate immunity and baseline microglial activation states can have biological consequences for brain function and do have consequences for immune surveillance of the brain's cellular health, phagocytosis of cellular components, and altered inflammatory responses to subsequent insults in many models (Tremblay and Majewska, 2011; Ji et al., 2013; Schafer et al., 2013). In the studies by Klein et al. (2016), decreased microglial activation correlated with decreased neurogenesis in the hippocampus. In our study, the consequences of modifying the baseline innate immune state in brain regions regulating respiratory control can only be speculated at this point (Feldman and Kam, 2015; Smith et al., 2013). However, the similarity of the changes in our study with those triggered by endotoxin tolerance may suggest that the changes observed here have a similar desensitizing function. Namely, to reduce the toxic effects of similar allergic challenges at subsequent time points on critical brain regions such as the brainstem regions controlling respiration.

Acknowledgments

The authors thank Yue Lin, Elma Frias, and Shaida Abachi for technical assistance and scientific discussions.

Declaration of Conflicting Interests

The author(s) declared no potential conflicts of interest with respect to the research, authorship, and/or publication of this article.

Funding

The author(s) disclosed receipt of the following financial support for the research, authorship, and/or publication of this article: This study was funded by grants from the University of California, Riverside Office of Research Seed grant (to D. L.) and from the National Institutes of Health (R01 AI63426 [to D. L.], R01 AI091759 [to M. G. N.], and R01 AG048099 [to M. J. C.]).

References

- Allan, A. L., & Keeney, M. (2010). Circulating tumor cell analysis: Technical and statistical considerations for application to the clinic. *J Oncol*, *2010*, 426218. doi: 10.1155/2010/426218
- Andersson, M., Downs, S., Mitakakis, T., Leuppi, J., & Marks, G. (2003). Natural exposure to *Alternaria* spores induces allergic rhinitis symptoms in sensitized children. *Pediatr Allergy Immunol*, *14*, 100–105.
- Barnewall, R. E., Benson, E. M., Brown, M. A., Fisher, D. A., Lindsay, A. S., Simmons, A. A., & Anderson, M. S. (2015). Characterization of a large animal aerosol exposure system for aerosolizing four strains of *Burkholderia pseudomallei*. *J Aerosol Sci*, *84*, 21–38.
- Bilbo, S. D., Block, C. L., Bolton, J. L., Hanamsagar R., & Tran P. K. (2018). Beyond infection—Maternal immune activation by environmental factors, microglial development and relevance for autism spectrum disorders. *Exp Neurol*, pii, S0014-4886(17)30176-0. doi:10.1016/j.expneurol.2017.07.002.
- Bonam, R., Partidos, C. D., Halmuthur, S. K. M., & Muller, S. (2017). An overview of novel adjuvants designed for improving vaccine efficacy. *Trends Pharmacol Sci*, *38*, 771–793.
- Bush, R. K., & Prochnau, J. J. (2004). *Alternaria*-induced asthma. *J Allergy Immunol*, *113*, 227–234.
- Calderón-Garcidueñas, L., Leray, E., Heydarpour, P., Torres-Jardón, R., & Reis, J. (2016). Air pollution, a rising environmental risk factor for cognition, neuroinflammation and neurodegeneration: The clinical impact on children and beyond. *Rev Neurol*, *172*, 69–80.
- Carson, M. J., Doose, J. M., Melchior, B., Schmid, C. D., & Ploix, C. C. (2006). CNS immune privilege: Hiding in plain sight. *Immunol Rev*, *13*, 48–65.
- Chen, G., Wang, S. H., Jang, J. C., Odegaard, J. I., & Nair, M. G. (2016). Comparison of RELM α and RELM β single- and double-gene-deficient mice reveals that RELM α expression dictates inflammation and worm expulsion in hookworm infection. *Infect Immun*, *84*, 1100–1111.
- Cho, D.-I., Kim, M. R., Jeong, H. Y., Jeong, M. H., Yoon, S. H., Kim, Y. S., & Ahn, Y. (2014). Mesenchymal stem cells reciprocally regulate the M1/M2 balance in mouse bone marrow-derived macrophages. *Exp Mol Med*, *46*, e70. doi: 10.1038/emm.2013.135.
- Cole, T. B., Coburn, J., Dao, K., Roque, P., Chang, Y. C., Kalia, V., Guilarte, T. R., Dziedzic, J., & Costa, L. G. (2016). Sex and genetic differences in the effects of acute diesel exhaust exposure on inflammation and oxidative stress in mouse brain. *Toxicology*, *374*, 1–9.

- Collins, P. E., & Carmody, R. J. (2015). The regulation of endotoxin tolerance and its impact on macrophage impact. *Crit Rev Immunol*, *35*, 293–323.
- Croston, T. L., Lemons, A. R., Beezhold, D. H., & Green B. J. (2018). MicroRNA regulation of host immune responses following fungal exposure. *Front Immunol*, *9*, 170. doi: 10.3389/fimmu.2018.00170
- Cunningham, C. (2013). Microglia and neurodegeneration: The role of systemic inflammation. *Glia*, *61*, 71–90. doi:10.1002/glia.22350
- Czirr, E., & Wyss-Coray, T. (2012). The immunology of neurodegeneration. *J Clin Invest*, *122*, 1156–1163.
- Dockery, D. W., Pope, C. A., Xu, X., Spengler, J. D., Are, J. H., Fay, M. E., Ferris, B. G., & Speizer, F. E. (1993). An association between air pollution and mortality in six US cities. *New Engl J Med*, *329*, 1753–1759.
- Doherty, T. A., Khorram, N., Sugimoto, K., Sheppard, D., Rosenthal, P., Cho J. Y., Pham, A., Miller, M., Croft, M., & Broide, D. H. (2012). *Alternaria* induces STAT6-dependent acute airway eosinophilia and epithelial FIZZ1 expression that promotes airway fibrosis and epithelial thickness. *J Immunol*, *188*, 2622–2629.
- Feldman, J. L., & Kam, K. (2015). Facing the challenge of mammalian neural microcircuits: Taking a few breaths may help. *J Physiol*, *593*, 3–23.
- Gabriel, M. F., Postigo, I., Tomaz, C. T., & Martínez, J. (2016). *Alternaria* alternate allergens: Markers of exposure, phylogeny and risk of fungi-induced respiratory allergy. *Environ Int*, *89–90*, 71–80.
- Gackiere, F., Saliba, L., Baude, A., Bosler, O., & Strube, C. (2011). Ozone inhalation activates stress-responsive regions of the CNS. *J Neurochem*, *117*, 961–972
- Ghosh, S., Hoselton, S. A., Dorsam, G. P., & Schuh, J. M. (2013). Eosinophils in fungus-associated allergic pulmonary disease. *Front Pharmacol*, *4*, 8. doi: 10.3389/fphar.2013.00008.
- Gold, D. R. (2017). NIAID, NIEHS, NHLBI, and MCAN Workshop report: The indoor environment and childhood asthma-implications for home environmental intervention in asthma prevention and management. *J Allergy Clin Immunol*, *140*, 933–949. doi: 10.1016/j.jaci.2017.04.024.
- Gordon, S. (2003). Alternative activation of macrophages. *Nat Rev Immunol*, *3*, 23–35.
- Guo, R. B., Sun, P. L., Zhao, A. P., Gu, J., Ding, X., Qi, J., Sun, X. L., & Hu, G. (2013). Chronic asthma results in cognitive dysfunction in immature mice. *Exp Neurol*, *247*, 209–217.
- Halonen, M., Stern, D. A., Wright, A. L., Taussiq, L. M., & Martinez, F. D. (1997). *Alternaria* as a major allergen for asthma in children raised in a desert environment. *Am J Resp Crit Care Med*, *155*, 1356–1361.
- Hering, S. V., Flagan, R. C., & Friedlander, S. K. (1978). Design and evaluation of new low-pressure impactor. I. *Environ Sci Technol*, *12*, 667–673.
- Hernandez, A., Donovan, V., Grinberg, Y. Y., Obenaus, A., & Carson, M. J. (2016). Differential detection of impact site versus rotational site injury by MRI and microglial morphology in an unrestrained mild closed head injury model. *J Neurochem*, *136* Suppl 1, 18–28.
- Heusinkveld, H. J., Wahle, T., Campbell, A., Westerink, R. H. S., Tran, L., Johnston, H., Stone, V., Cassee, F. R., & Schins, R. P. F. (2016). Neurodegeneration and neurological disorders by small inhaled particles. *Neurotoxicology*, *56*, 94–106.
- Jayaraj, R. L., Rodriguez, E. A., Wang, Y., & Block, M. L. (2017). Outdoor ambient air pollution and neurodegenerative diseases: The neuroinflammation hypothesis. *Curr Environ Health Rep*, *4*, 166–179.
- Ji K., Miyauchi J., & Tsirka S. E. (2013). Microglia: An active player in the regulation of synaptic activity. *Neural Plast*, *2013*, 627325.
- Kader R., Kennedy K., & Portnoy J. M. (2018). Indoor environmental interventions and their effect on asthma outcome. *Curr Allergy Asthma Rep*, *18*, 17. doi: 10.1007/s11882-018-0774-x.
- Klein, B., Mrowetz, H., Thalhamer, J., Scheibhofer, S., Weiss, R., & Aigner, L. (2016). Allergy enhances neurogenesis and modulates microglial activation in the hippocampus. *Front Cell Neurosci*, *10*, 169. doi: 10.3389/fncel.2016.00169
- Knutsen, A. P., Bush, R. K., Demain, J. G., Denning, D. W., Dixit, A., Fairs, A., Greenberger, P. A., Kariuki, B., Kita, H., Kurup, V. P., Moss, R. B., Niven, R. M., Pashley, C. H., Slavin, R. G., Vijay, H. M., & Wardlaw, A. J. (2012). Fungi and allergic lower respiratory tract diseases. *J Allergy Clin Immunol*, *129*(2), 280–291.
- Ko, M. T., Huang, S. C., & Kang, H. Y. (2015). Establishment and characterization of an experimental mouse model of allergic rhinitis. *Eur Arch Oto-Rhino-Laryngol*, *272*, 1149–1155.
- Kodavanti, P. R., Royland, J. E., Richards, J. E., Besas, J., & Macphail, R. C. (2011). Toluene effects on oxidative stress in brain regions of young-adult, middle-age, and senescent Brown Norway rats. *Toxicol Appl Pharmacol*, *256*, 386–398.
- Kodavanti, U. P., Schladweiler, M. C., Ledbetter, A. D., Watkinson, W. P., Campen, M. J., Winsett, D. W., Richards, J. R., Crissman, K. M., Hatch, G. E., & Costa, D. L. (2000). The spontaneously hypertensive rat as a model of human cardiovascular disease: Evidence of exacerbated cardiopulmonary injury and oxidative stress from inhaled emission particulate matter. *Toxicol Appl Pharmacol*, *164*, 250–263.
- Kubo, M. (2017). Innate and adaptive type 2 immunity in lung allergic inflammation. *Immunol Rev*, *278*, 162–172.
- Kumar, V., Abbas, A. K., & Aster, J. C. (2014). *Robbins & Cotran pathologic basis of disease* (9th ed.). London, England: Elsevier Health Science.
- Levesque, S., Taetzsch, T., Lull, M. E., Kodavanti, U., Stadler, K., Wagner, A., Johnson, J. A., Duke, L., Kodavanti, P., Surace, M. J., & Block, M. L. (2011). Diesel exhaust activates and primes microglia: Air pollution, neuroinflammation, and regulation of dopaminergic neurotoxicity. *Environ Health Perspect*, *119*, 1149–1155.
- Ljubimova, J. Y., Braubach, O., Patil, R., Chiechi, A., Tang, J., Galstyan, A., Shatalova, E. S., Kleinman, M. T., Black, K. L., & Holler, E. (2018). Coarse particulate matter (PM_{2.5-10}) in Los Angeles Basin air induces expression of inflammation and cancer biomarkers in rat brains. *Sci Rep*, *8*, 5708. doi: 10.1038/s41598-018-23885-3.
- May, K. R. (1973). The collision nebulizer: Description, performance and application. *J Aerosol Sci*, *4*, 235–238, IN1, 239–243.

- McDonald, J. D., Doyle-Eisele, M., Campen, M. J., Seagrave, J., Homes, T., Lund, A., Surratt, J. D., Seinfeld, J. H., Rohr, A. C., & Knipping, E. M. (2010). Cardiopulmonary response to inhalation of biogenic secondary organic aerosol. *Inhal Toxicol*, *22*, 253–265.
- Mulholland, G. W., Donnelly, M. K., Hagwood, C. R., Kukuck, S. R., Hackley, V. A., & Pui, D. Y. (2006). Measurement of 100 nm and 60 nm particle standards by differential mobility analysis. *J Res Natl Inst Stand Technol*, *111*, 257–312.
- Mumaw, C. L., Levesque, S., McGraw, C., Robertson, S., Lucas, S., Stafflinger, J. E., Campen, M. J., Hall, P., Norenberg, J. P., Anderson, T., Lund, A. K., McDonald, J. D., Ottens, A. K., & Block, M. L. (2016). Microglial priming through the lung-brain axis: The role of air pollution-induced circulating factors. *FASEB J*, *30*, 1880–1890.
- Munder, M., Eichmann, K., & Modolell, M. (1998). Alternative metabolic states in murine macrophages reflected by the nitric oxide synthase/arginase balance: Competitive regulation by CD4⁺ T cells correlates with Th1/Th2 phenotype. *J Immunol*, *160*, 5347–5354.
- Nomura, F., Akashi, S., Sakao, Y., Sato, S., Kawai, T., Matsumoto, M., Nakanishi, K., Kimoto, M., Miyake, K., Takeda, K., & Akira, S. (2000). Cutting edge: Endotoxin tolerance in mouse peritoneal macrophages correlates with down-regulation of surface toll-like receptor 4 expression. *J Immunol*, *164*, 3476–3479.
- Pena, O. M., Pistollic, J., Raj, D., Fjell, C. D., & Hancock, R. E. (2011). Endotoxin tolerance represents a distinctive state of alternative polarization (M2) in human mononuclear cells. *J Immunol*, *186*, 7243–7254.
- Perry, V. H. (2010). Contribution of systemic inflammation to chronic neurodegeneration. *Acta Neuropathol*, *120*, 277–286. doi:10.1007/s00401-010-0722-x
- Ploix, C., Zuberi, R. I., Liu, F. T., Carson, M. J., & Lo, D. D. (2009). Induction and effector phase of allergic lung inflammation is independent of CCL21/CCL19 and LT-beta. *Int J Med Sci*, *6*, 85–92.
- Ploix, C. C., Noor, S., Crane, J., Masek, K., Carter, W., Lo, D. D., Wilson, E. H., & Carson, M. J. (2011). CNS-derived CCL21 is both sufficient to drive homeostatic CD4⁺ T cell proliferation and necessary for efficient CD4⁺ T cell migration into the CNS parenchyma following *Toxoplasma gondii* infection. *Brain Behav Immun*, *25*, 883–896.
- Pope, C. A., Burnett, R. T., Thun, M. J., Calle, E. E., Krewski, D., Ito, K., & Thurston, G. D. (2002). Lung cancer, cardiopulmonary mortality, and long-term exposure to fine particulate air pollution. *JAMA*, *287*, 1132–1141.
- Raaschou-Nielsen, O., et al. (2013). Air pollution and lung cancer incidence in 17 European cohorts: Prospective analyses from the European Study of Cohorts for Air Pollution Effects (ESCAPE). *Lancet Oncol*, *14*, 813–822.
- Rajaiah, R., Perkins, D. J., Polumuri, S. K., Zhao, A., Keegan, A. D., & Vogel, S. N. (2013). Dissociation of endotoxin tolerance and differentiation of alternatively activated macrophages. *J Immunol*, *190*, 4763–4772.
- Rosenbaum, M. D., Van de Woude, S., & Johnson, T. E. (2009). Effects of cage-change frequency and bedding volume on mice and their microenvironment. *J Am Assoc Lab Animal Sci*, *48*, 763–773.
- Roy, C. J., Hale, M., Hartings, J. M., & Pitt, L. (2003). Impact of inhalation exposure modality and particle size on the respiratory deposition of ricin in BALB/C mice. *Inhal Toxicol*, *15*, 619–638.
- Roy, C. J., & Pitt, L. M. (2006). Infectious disease aerobiology: Aerosol challenge methods. In J. R. Swearingen (Ed.), *Biodefense: Research methodology and animal models*. Boca Raton, FL: CRC Press.
- Sarlus, H., Wang, X., Cedazo-Minguez, A., Schultzberg, M., & Oprica, M. (2013). Chronic airway-induced allergy in mice modifies gene expression in the brain toward insulin resistance and inflammatory responses. *J Neuroinflammation*, *10*, 99. doi:10.1186/1742-2094-10-99
- Smith, J. C., Abdala, A. P. L., Borgmann, A., Rybak, I. A., & Paton, J. F. R. (2013). Brainstem respiratory networks: Building blocks and microcircuits. *Trends Neurosci*, *36*, 152–162.
- Schafer, D. P., Lehrman, E. K., & Stevens, B. (2013). The “quad-partite” synapse: Microglia-synapse interactions in the developing and mature CNS. *Glia*, *61*, 24–36.
- Schmid, C. D., Melchior, B., Masek, K., Puntambeker, S. S., Danielson, P. E., Lo, D. D., Sutcliffe, J. G., Carson, M. J. (2009). Differential gene expression in LPS/IFN γ activated microglia and macrophages: In vitro versus in vivo. *J Neurochem*, *109* Suppl 1, 117–125.
- Tremblay, M. È., & Majewska, A. K. (2011). A role for microglia in synaptic plasticity? *Commun Integr Biol*, *4*, 220–222.
- Vianello, A., Caminati, M., Crivellaro, M., El Mazloum, R., Sneghi, R., Schiappoli, M., Dama, A., Rossi, A., Festi, G., Marchi, M. R., Bovo, C., Canonica, G. W., & Senna, G. (2016). Fatal asthma: Is it still an epidemic? *World Allergy Organ J*, *9*, 42. doi: 10.1186/s40413-016-0129-9.
- Wang, S. C., & Flagan, R. C. (1990). Scanning electrical mobility spectrometer. *Aerosol Sci Technol*, *13*, 230–240.
- Xia, M. X., Ding, X., Qi, J., Gu, J., Hu, G., & Sun, X. L. (2014). Inhaled budesonide protects against chronic asthma induced neuroinflammation in mouse brain. *J Neuroimmunol*, *273*, 53–57.
- Yamasaki, R., Fujii, T., Wang, B., Masaki, K., Kido, K. A., Yshida M., Matsushita T., Kira J. (2016). Allergic inflammation leads to neuropathic pain via glial cell activation. *J Neurosci*, *36*, 11929–11945.
- Ye, J., Salehi, S., North, M. L., Portelli, A., Chow, C. W., & Chan, A. W. (2017). Development of a novel simulation reactor for chronic exposure to atmospheric particulate matter. *Sci Rep*, *7*, 42317.
- Zhou, W., Toki, S., Zhang, J., Goleniewksa, K., Newcomb, D. C., Cephus, J. Y., Dulek, D. E., Bloodworth, M. H., Stier, M. T., Polosuhkin, V., Gangula, R. D., Mallal, S. A., Broide, D. H., & Peebles, R. S., Jr. (2016). Prostaglandin I₂ signaling and inhibition of group 2 innate lymphoid cell responses. *Am J Respir Crit Care Med*, *93*, 31–42.